Research Square

Preprints are preliminary reports that have not undergone peer review.
They should not be considered conclusive, used to inform clinical practice,
or referenced by the media as validated information.

Freezing Storage Prior to Processing Preserves Flavor and Nutritional Quality of Vacuum-Packed Sweet Corn

Hua Chen
Beijing Academy of Agricultural and Forestry Sciences
jinhua zuo
Beijing Academy of Agricultural and Forestry Sciences
Yunxiang Wang
Beijing Academy of Agricultural and Forestry Sciences
Xinyuan Zhou
Beijing Academy of Agricultural and Forestry Sciences
Tianyu Li
Beijing Academy of Agricultural and Forestry Sciences
Xu Liu
Beijing Academy of Agricultural and Forestry Sciences
Chunmei Bai
Beijing Academy of Agricultural and Forestry Sciences
Jiejie Tao
Beijing Academy of Agricultural and Forestry Sciences
Xinyi Feng
Beijing Academy of Agricultural and Forestry Sciences
Yiting Ren
Beijing Academy of Agricultural and Forestry Sciences
Ronghuan Wang
Beijing Academy of Agricultural and Forestry Sciences
Yaxing Shi
Beijing Academy of Agricultural and Forestry Sciences
Lihong Wang
Hebei University of Engineering
Yanyan Zheng
jxzhengyanyan@163.com

Beijing Academy of Agricultural and Forestry Sciences

Article

Keywords:

Posted Date: February 20th, 2026

DOI: https://doi.org/10.21203/rs.3.rs-8853808/v1

License: This work is licensed under a Creative Commons Attribution 4.0 International License.
Read Full License

Additional Declarations: No competing interests reported.

Abstract

Sweet corn deteriorates rapidly postharvest, creating challenges for continuous industrial processing. Freezing storage prior to processing (IQFP) is widely used, yet its mechanistic effects on product quality remain unclear. Here, sensory evaluation, texture profiling, color analysis, flavor omics, and metabolomics were integrated to compare IQFP with immediate postharvest processing in vacuum-packed sweet corn during 120 days of storage. Although both treatments showed similar quality once processed after the freezing stage, IQFP maintained significantly higher sensory scores during prolonged storage, delaying rancid flavor development and reducing color fading. IQFP produced a more desirable texture with lower cohesiveness and moderate hardness. Aroma analysis showed reduced accumulation of lipid-oxidation-derived off-flavor compounds while preserving key Maillard-derived odorants. Metabolomics revealed enhanced accumulation of protective sugars, slower sucrose degradation, and reduced oxidative-stress-associated metabolites. Together, IQFP improves flavor stability and metabolic resilience, supporting its use to stabilize product quality and alleviate peak-harvest processing pressure.

Introduction

Sweet corn (*Zea mays* L.) is harvested at the milk stage and consumed as fresh cobs or processed products, valued for its high nutritional quality, distinctive flavor, and strong economic return[1]. It is widely cultivated worldwide, and in China the planting area now exceeds 6 million mu. However, production is constrained by a short and highly seasonal harvest window combined with heavy reliance on manual harvesting, creating substantial processing pressure. sweet corn has high moisture content and intense postharvest respiration, leading to rapid deterioration manifested as texture toughening, decay, sweetness loss[2], and flavor degradation caused by depletion of key taste compounds (e.g., sugars and amino acids) and volatile aroma constituents (e.g., aldehydes and ketones)[3–5]. Its shelf life typically ranges from 3 to 5 days, making year-round supply difficult[6]. During peak harvest, large volumes enter the market simultaneously, while processing capacity cannot match the rate of postharvest deterioration, resulting in considerable economic losses.

Vacuum-packed sweet corn (VPSC) has emerged as an effective strategy to address these constraints due to its ready-to-eat nature, extended shelf life, and convenience in storage and distribution[7–8]. Vacuum processing reduces oxygen availability and microbial activity, enabling several months of ambient storage without chemical preservatives[9]. Previous studies have shown that vacuum packaging suppresses oxidative reactions and preserves major nutrients, including proteins, carbohydrates, and dietary fiber, with particularly strong retention of lipid-soluble vitamins and carotenoids[10]. However, with rapid expansion of cultivation scale, conventional immediate postharvest processing (VAC) increasingly fails to meet capacity demands during peak harvest. Substantial deterioration can occur while raw corn awaits processing, forcing factories to operate under overload conditions and resulting in unstable product quality.

Freezing storage prior to processing (IQFP) offers a practical solution. Rapid freezing enables quick passage through the critical ice-crystal formation zone, slowing physiological metabolism and delaying sugar conversion and degradation of volatile flavor compounds[11–13]. Although ice-crystal formation may induce cellular damage and drip loss during thawing, most flavor precursors remain preserved[12, 14]. Studies in frozen fruits and vegetables indicate minimal effects on core nutrients such as proteins, carbohydrates, and minerals, with nutritional value close to that of fresh materials[15]. Freezing therefore extends raw material storage life[16], alleviates processing pressure during concentrated harvest periods, and enables staggered processing, supporting year-round production of VPSC with stable quality.

Despite these advantages, systematic understanding of how IQFP influences flavor and nutritional quality of processed sweet corn during storage remains limited. In this study, HS-SPME-GC-MS and GC-IMS were integrated with widely targeted and targeted metabolomics to compare dynamic changes in flavor and nutritional quality of VPSC produced by VAC and IQFP. The underlying mechanisms by which IQFP enhances storage stability were elucidated, providing a technological basis for mitigating peak-harvest processing pressure, improving product uniformity, and enhancing the commercial value of the sweet corn industry.

Results

Effects of processing methods on sensory evaluation and color of VPSC

At the early storage stage (30 days), VAC and IQFP samples showed comparable overall acceptability, both maintaining desirable sensory quality characterized by bright color, plump kernels, and a sweet aroma (Fig. 1a). During prolonged storage, sensory scores declined in both groups, but deterioration occurred more rapidly in VAC. By 120 d, the overall score of VAC decreased to 58, accompanied by dull color, reduced kernel elasticity, and detectable rancid odor and browning, indicating severe quality loss. In contrast, IQFP maintained a score of 74, with superior color retention, texture stability, and flavor preservation, remaining within the acceptable sensory range and demonstrating greater storage stability.

Over 120 days, the lightness value (L^*) increased significantly in VPSC, consistent with a progressively paler appearance (Fig. 1g). This change is likely associated with moisture migration, structural rearrangement, and starch retrogradation. VAC consistently showed higher L^* values than IQFP. The absolute value of a^* gradually decreased, with a smaller reduction in IQFP, while b^* increased more rapidly in VAC, indicating a color shift toward the yellow-red quadrant (Fig. 1h-i). However, because the increase in L^* was dominant, overall color saturation declined. IQFP more effectively suppressed abnormal brightness increase and pigment degradation, resulting in the smallest deviation from CK-0d after 120 days and indicating improved resistance to color fading during long-term storage.

Effects of processing methods on texture properties of VPSC

Texture profile analysis revealed distinct differences in texture evolution between treatments. After 30 d, hardness in VAC-30d (33.04 N) was slightly higher than CK-0d (31.14 N), whereas IQFP-30d showed significantly lower hardness (15.18 N) (Fig. 1b). Cohesiveness, springiness, and chewiness in VAC-30d were also higher than CK-0d, indicating a relatively compact structure. In contrast, IQFP-30d displayed generally lower values, reflecting initial softening likely induced by freeze–thaw-related tissue disruption.

During prolonged storage (30-120 d), hardness, springiness, chewiness, and total work in VAC increased continuously, peaking at 90 days (Fig. 1c-f). In IQFP samples, hardness gradually recovered after cooking, accompanied by moderate increases in springiness, chewiness, and total work, but values remained significantly lower than those of VAC at corresponding time points ($p < 0.05$) and no peak pattern was observed. Notably, at 120 days, IQFP exhibited the lowest cohesiveness (0.45) among all groups. Combined with its relatively lower hardness, this indicates the formation of a looser, more chewable texture. Overall, VAC developed excessive hardness and toughness during long-term storage, impairing eating quality, whereas IQFP showed moderated texture evolution and improved palatability despite initial freeze–thaw softening.

Electronic nose-based flavor profile discrimination

Electronic nose radar plots revealed distinct volatile response patterns between VAC and IQFP samples across storage time (Fig. 2a, c). Sensors W1W (sulfur-organic), W5S (broad-range), W1S (broad-methane), and W2S (broad-alcohol) exhibited generally higher responses than other sensors. W1W showed strong responses in both treatments, with the highest value in VAC-120d (18.50). W5S reached maximum responses in IQFP-60d (14.57) and IQFP-120d (14.37), indicating increasing flavor complexity under IQFP (Fig. 2b). W2S peaked in VAC-120d (13.12), suggesting pronounced accumulation of alcohol-related volatiles in VAC.

During storage, IQFP showed an initial increase followed by stabilization in W5S, W1W, and W2S responses, while W1S remained relatively stable except at 90 days, indicating sustained formation and retention of volatile classes and a more continuous flavor profile. In contrast, VAC exhibited higher early responses followed by decline at 60–90 days and a sharp increase at 120 days, reflecting greater late-stage flavor fluctuation. Principal component analysis (PCA) and linear discriminant analysis (LDA) further confirmed these differences. PCA showed that PC1 and PC2 explained 90.54% of total variance, sufficiently representing the overall volatile profile (Fig. 2d). IQFP and VAC samples were clearly separated, indicating distinct flavor characteristics between processing methods. IQFP samples clustered tightly along PC1, demonstrating higher flavor consistency, whereas VAC samples were more dispersed along PC2, indicating greater variability. LDA identified W1W, W5S, W1S, and W2S as the primary discriminative sensors, consistent with radar plot observations (Fig. 2e).

Effects of processing methods on flavor fingerprint of VPSC during storage

Based on GC-IMS flavor fingerprinting with CK-0d as reference, dynamic changes in volatile compounds were compared between treatments throughout storage (Fig. 3a). At the early storage stage, VOCs associated with fresh fruity and herbal notes—including hexyl acetate, ethyl benzoate, benzyl alcohol, (E)-2-hexenal, and terpenes such as camphene, myrcene, p-cymene, and borneol—were more abundant in VAC. However, during prolonged storage, lipid-oxidation markers such as (E,E)-2,4-nonadienal (rancid odor), together with 2-pentylfuran and oct-1-en-3-ol (beany/green/mushroom notes), increased markedly in VAC, and trace levels of 2,4,5-trichlorophenol were detected. These results indicate that although VAC initially preserved fresh floral–fruity aromas, it exhibited poorer oxidative stability during long-term storage, leading to flavor deterioration and potential contamination risk.

In contrast, IQFP showed superior flavor stability (Fig. 3b). Although early levels of some VOCs (e.g., ethyl benzoate) were slightly lower than in VAC, IQFP suppressed accumulation of off-flavor compounds such as 1-hydroxy-2-propanone and oct-1-en-3-ol during middle and late storage. The increase in (E,E)-2,4-nonadienal was significantly lower in IQFP, and contaminants including 2,4,5-trichlorophenol and thiocyanic acid methyl ester were not detected. Moreover, IQFP retained higher levels of Maillard-derived aroma compounds such as 2-acetyl-1-pyrroline, 2-acetylfuran, 2,5-dimethylpyrazine, trimethylpyrazine, 2-ethylpyrazine, and furfural (Supplementary Table S1). This likely reflects reduced enzymatic and microbial activity during frozen storage, preserving flavor precursors and supporting a more complex and stable aroma profile during subsequent processing and storage. Overall, IQFP enhanced oxidative stability, preserved intrinsic flavor quality, and reduced off-flavor formation during long-term storage.

Identification of differential volatile metabolites (DVMs) based on HS-SPME-GC-MS

Overlay analysis of total ion chromatograms from quality control (QC) samples showed highly consistent spectral patterns, confirming stable instrument performance (Supplementary Fig. S1). The proportion of DVMs with coefficient of variation (CV) < 0.3 exceeded 75% in CK-0d, VAC-120d, and IQFP-120d, while compounds with CV < 0.5 exceeded 85% in VAC-30d and IQFP-30d, indicating high data reliability (Supplementary Fig. S2). Correlation analysis further demonstrated strong biological reproducibility within groups ($|r| > 0.92$). CK-0d, VAC-30d, IQFP-30d, and IQFP-120d showed strong positive correlations ($|r| > 0.81$), whereas VAC-120d exhibited weaker correlation with other groups (as low as 0.37), reflecting substantial divergence in volatile composition (Supplementary Fig. S3).

A total of 873 volatile compounds were identified, including 156 esters, 129 terpenes, 114 ketones, 100 heterocyclic compounds, 84 alcohols, 66 aldehydes, 64 hydrocarbons, 40 acids, 34 amines, 30 phenols, 20 nitrogen-containing compounds, 15 aromatics, 11 ethers, 6 sulfur compounds, and 4 halogenated hydrocarbons (Supplementary Fig. S4). CK-0d contained 298.80 μg/mL total volatiles, dominated by ketones (34.46%) and terpenes (17.20%) (Fig. 4a). After short-term storage (30 d), total volatiles increased, with IQFP-30d (305.13 μg/mL) and VAC-30d (309.06 μg/mL) showing similar levels, mainly ketones and heterocyclic compounds. DVMs between IQFP-30d and VAC-30d were enriched in

biosynthesis of secondary metabolites, benzoxazinoid biosynthesis, phenylpropanoid biosynthesis, monoterpenoid biosynthesis, and phenylalanine/tyrosine/tryptophan biosynthesis, indicating active precursor formation for flavor development (Supplementary Fig. S5a).

After long-term storage (120 d), treatment differences became more pronounced. IQFP-120d remained dominated by ketones (36.43%) and heterocyclic compounds (17.13%), with the lowest total volatile concentration (258.66 μg/mL), slightly below CK-0d. In contrast, VAC-120d exhibited a marked increase in total volatiles (408.06 μg/mL), primarily heterocyclic compounds and ketones. DVMs between IQFP-120d and VAC-120d were enriched in tryptophan metabolism, benzoxazinoid biosynthesis, and secondary metabolite biosynthesis (Supplementary Fig. S5b). These findings indicate minimal flavor differences at 30 days but substantial divergence at 120 days, with VAC generating numerous new volatiles while IQFP showed moderated decline and greater stability (Supplementary Table S2).

Relative odor activity value (ROAV) analysis

ROAV analysis identified key aroma contributors among 277 compounds, of which 187 differed between groups. At 30 days, despite similar total volatile concentrations, key aroma profiles differed. Dihydro-2-methyl-3(2H)-furanone, 1-nonen-3-one, 1-hexen-3-one, and 1-octen-3-one consistently showed high ROAV values, forming the dominant sweet, mushroom, and cooked-vegetable aroma base (Fig. 4b). Higher ROAV values of dihydro-2-methyl-3(2H)-furanone, (Z)-3-hexenal, and 1-hexen-3-one in IQFP-30d contributed to stronger sweet and green notes (Fig. 4c). Conversely, S-ethyl ethanethioate, 1,2-dithiane, and (E,E)-2,4-decadienal were more prominent in VAC-30d, contributing onion-, garlic-, and earthy-like odors. Notably, 4-methyl-5-thiazoleethanol (roasted/meaty note) was detected only in CK-0d and IQFP-30d, indicating better preservation of characteristic aroma in IQFP.

After 120 days, aroma divergence became pronounced. The ROAV of 1-nonen-3-one increased sharply in VAC-120d, intensifying mushroom-like notes. Unsaturated aldehydes associated with rancid and oxidative off-flavors accumulated markedly in VAC-120d, with (E,E)-2,4-decadienal and (E,E)-2,4-nonadienal reaching 13.7- and 13.6-fold higher levels than in IQFP-120d, respectively. Sulfurous and fecal odor compounds, including S-ethyl ethanethioate and 3-methylindole, were also significantly higher. Additionally, 2-pentylpyridine, a key lipid-oxidation marker, showed a 29-fold higher ROAV in VAC-120d (Supplementary Table S3). These results indicate that VAC is more susceptible to flavor deterioration during prolonged storage, whereas IQFP effectively suppresses off-flavor formation and preserves intrinsic aroma characteristics.

Aroma flavor wheel construction and analysis

To visualize sensory differences, aroma wheels were constructed for 30 and 120 days (Fig. 4d-e). At 30 days, aroma profiles of IQFP and VAC were highly similar, with 107 annotated attributes. Green, sweet, and fruity were the dominant categories, each associated with multiple compounds. Additional attributes

—including woody, fatty, waxy, herbal, nutty, balsamic, and floral—were linked to several differential volatiles, indicating that early storage differences primarily affected fresh and sweet aroma components while maintaining a similar overall profile.

At 120 days, aroma divergence became evident, with 130 annotated attributes. The number of DVMs contributing to green, fruity, sweet, and fatty attributes increased markedly, while undesirable attributes such as sulfury, animalic, meaty, musty, earthy, and soapy emerged, reflecting accumulation of off-flavor compounds. Overall, flavor shifted from fresh fruity–sweet notes toward stronger rancid and fatty characteristics during prolonged storage. However, IQFP exhibited the fewest undesirable attributes and associated volatiles, demonstrating superior storage stability and flavor retention compared with VAC.

Differential sugar composition during storage

To clarify the chemical basis of sweetness changes in VPSC during storage, dynamic variations in key soluble sugars were quantified. Data quality assessed by the empirical cumulative distribution function of coefficients of variation showed that more than 80% of analytes had CV values < 0.2 and < 0.3, indicating high analytical stability (Fig. 5a).

After 30 days, sucrose declined from 132.02 mg/g in fresh VPSC to 101.02 mg/g in VAC-30d and 105.72 mg/g in IQFP-30d. Meanwhile, glucose increased from 3.58 mg/g to approximately 20 mg/g in both groups, and D-fructose rose from 2.52 mg/g to 8.92 mg/g (VAC-30d) and 13.13 mg/g (IQFP-30d). Maltose and D-(+)-cellobiose accumulated to higher levels in IQFP-30d, suggesting active sucrose hydrolysis accompanied by starch and/or cellulose degradation during early storage (Fig. 5b-c).

By day 120, sucrose further decreased to 43.65 mg/g in VAC-120d, accompanied by marked accumulation of glucose (38.02 mg/g) and D-fructose (24.00 mg/g). In contrast, sucrose hydrolysis was substantially attenuated in IQFP-120d, where sucrose remained at 86.55 mg/g—approximately 2.0-fold higher than VAC-120d—while glucose (23.67 mg/g) and D-fructose (15.65 mg/g) accumulated to lower levels. D-(+)-cellobiose and trehalose, associated with cell wall carbohydrate metabolism and stress protection, respectively, were also maintained at relatively higher levels in IQFP-120d (Supplementary Table S4). Collectively, these findings indicate that sweetness loss in VAC was associated with accelerated sucrose degradation and reducing sugar accumulation, whereas IQFP slowed sucrose breakdown and preserved cell wall–related carbohydrate components, contributing to improved sweetness retention and storage stability.

Widely targeted metabolomics analysis

To characterize metabolic alterations of VPSC during storage under different processing strategies, widely targeted metabolomics was performed. A total of 2,576 DAMs were detected, mainly including 350 lipids, 341 ketones/aldehydes/esters, 274 sugars, and 229 terpenoids (Supplementary Fig. S6). PCA

showed clear separation among treatment groups along PC1 (34.12%) and PC2 (26.27%), indicating pronounced metabolic divergence across processing methods and storage periods (Supplementary Fig. S7). Replicate correlation analysis further demonstrated high within-group consistency and lower between-group similarity, suggesting that different treatments substantially reshaped the metabolic landscape of VPSC during storage (Supplementary Fig. S8).

Differential accumulation metabolites (DAMs) patterns during short-term storage

In CK-0d vs VAC-30d, 1,684 DAMs were identified, including 679 Level-1 annotated compounds (>90% confidence), with 50.81% upregulated. DAMs were classified into 18 categories, dominated by sugars (12.2%), ketones/aldehydes/esters (11.6%), amino acids (10.6%), organic acids (10.2%), and lipids (8.5%) (Fig. 6a, c). KEGG enrichment revealed predominant involvement of arginine biosynthesis, D-amino acid metabolism, glyoxylate and dicarboxylate metabolism, lysine biosynthesis, and purine metabolism (Fig. 6b). Compared with CK-0d, VAC-30d exhibited accumulation of L-ornithine, myristoleic acid, and methylmalonic acid, while multiple umami-related amino acids and nitrogen-metabolism intermediates—including L-glutamic acid, L-arginine, L-aspartic acid, L-citrulline, L-glutamine, and 2-ketoglutaric acid—were significantly reduced (Fig. 6e). These patterns suggest depletion of umami-associated amino acids and accumulation of unsaturated fatty acids during early VAC storage, potentially accompanied by activation of endogenous stress-response pathways.

In IQFP-30d vs CK-0d, the number of DAMs decreased by 72 relative to CK-0d vs VAC-30d, and Level-1 DAMs decreased by 25. The proportions of sugars and organic acids declined to 10.55% and 7.95%, respectively, whereas lipids increased to 11.62%. In the zeatin biosynthesis pathway, trans-zeatin and its precursor trans-zeatin riboside increased markedly, together with cis-zeatin-7-N-glucoside (Fig. 6d). Purine metabolism was broadly upregulated, with hypoxanthine (+24.6-fold), xanthine (+3.4-fold), cyclic nucleotides, and adenosine significantly elevated. Similar to VAC-30d, certain umami-related amino acids such as L-aspartic acid declined; however, γ-aminobutyric acid (GABA), a stress-associated metabolite and potential taste enhancer, accumulated significantly, which may support favorable flavor development during storage.

Differential Metabolite Patterns during Long-Term Storage

In VAC-120d vs IQFP-120d, 1,648 DAMs were identified, including 931 upregulated and 717 downregulated metabolites. Major categories included ketones/aldehydes/esters (15.84%), lipids (14.62%), and sugars (11.59%) (Fig. 6a). KEGG enrichment analysis revealed that the DAMs during late storage were predominantly enriched in the critical metabolic pathways of purine metabolism and phenylalanine metabolism (Supplementary Fig. S9). IQFP-120d showed higher levels of D-(+)-trehalose, D-(+)-cellobiose, and DL-glyceric acid compared with VAC-120d. Notably, 13-hydroxy-9Z,11E-octadecadienoic acid (13-HODE), a lipid-derived metabolite with potential roles in flavor precursor

formation, was 4.5-fold higher in IQFP-120d. Rubinaphthin A, a bioactive secondary metabolite potentially associated with surface activity and antimicrobial effects, was 9.7-fold higher in IQFP-120d (Fig. 6e).

Conversely, VAC-120d accumulated higher levels of metabolites associated with bitterness and off-flavor formation, including hypoxanthine, phosphorylcholine, lysophosphatidylcholine (LysoPC 20:4), and phosphatidylethanolamine (16:1/18:0). Sinapinic acid and ferulic acid were also markedly enriched, compounds whose excessive accumulation has been linked to astringency and irritant sensory attributes (Supplementary Table S5). Overall, IQFP favored accumulation of stress-protective sugars, oxidized lipid-derived flavor precursors, and bioactive secondary metabolites during long-term storage, whereas VAC exhibited more pronounced membrane lipid degradation and oxidative progression, consistent with its inferior storage quality.

Discussion

Food flavor is a multidimensional trait arising from the interaction between biochemical processes and human sensory perception[17], integrating visual, gustatory, olfactory, and textural signals to shape the overall eating experience[18]. In corn, flavor quality is determined by the coordinated interplay of sweetness, aroma, texture, and color[19]. This study systematically compared long-term storage flavor quality of VPSC produced by VAC and IQFP, providing mechanistic insights from sensory, textural, flavoromic, and metabolomic perspectives into improving flavor stability in ready-to-eat food products.

Appearance strongly influences initial consumer acceptance, whereas odor and texture largely determine eating satisfaction[20]. After 120 days, IQFP maintained significantly higher sensory scores than VAC, in which rancid odor and browning had emerged. Texture profile analysis showed that hardness in IQFP decreased initially after thawing and then gradually increased. This behavior likely reflects the formation of small ice crystals during rapid freezing, which transiently weaken structural binding upon melting[21]. Although early softening reduces instrumental hardness, its sensory consequence is dual: perceived hardness may decrease temporarily, yet the structure becomes looser and more chewable during subsequent storage. In contrast, VAC exhibited marked increases in hardness and chewiness during mid-to-late storage, indicating excessive tissue hardening and reduced palatability. Slower starch retrogradation in IQFP contributed to more moderate increases in hardness and chewiness and lower cohesiveness, resulting in a more favorable texture. Meanwhile, VAC samples became progressively paler during storage. Although color differences between treatments were modest, visual cues may influence flavor perception through cross-modal sensory interactions, potentially amplifying negative perception when combined with textural deterioration[18].

Aroma generation in cooked corn is primarily driven by thermal reactions such as caramelization and the Maillard reaction, which produce characteristic volatile compounds[22]. The aroma profile of VPSC was dominated by high-ROAV volatiles including dihydro-2-methyl-3(2H)-furanone and 1-nonen-3-one,

forming a stable base of sweet, mushroom-like, and cooked-vegetable notes[23]. During prolonged storage, however, flavor deterioration in VAC was mainly associated with lipid oxidation. Oxidative markers such as (E,E)-2,4-nonadienal and off-flavor compounds including 2-pentylpyridine increased markedly, accompanied by elevated ROAV values of compounds contributing earthy, sulfurous, and fecal odor notes. This pattern resembles lipid-derived off-flavor formation reported in other stored plant tissues[24]. In contrast, IQFP retained higher levels of Maillard-derived characteristic aroma compounds such as 2-acetyl-1-pyrroline and trimethylpyrazine during late storage while suppressing undesirable volatiles such as 1-hydroxy-2-propanone and oct-1-en-3-ol, thereby stabilizing overall flavor quality.

Flavor perception arises from the integrated contribution of numerous volatile compounds[3], and aroma diversity is often more closely associated with consumer acceptance than intensity alone[25]. In early storage, both treatments were dominated by fresh green, sweet, and fruity notes. During late storage, VAC developed undesirable sulfurous, animal-like, and musty attributes, reflecting accumulation of associated volatiles and pronounced flavor deterioration. In contrast, IQFP maintained clearer roasted and nutty notes derived from Maillard products and preserved higher levels of fruity and sweet aroma-related compounds, suggesting that freezing suppressed lipid oxidation pathways and preserved flavor precursors for later stages of storage.

Sweetness has emerged as a key determinant of corn flavor and texture quality[19]. After 120 days, sucrose content in VAC declined to approximately half that in IQFP, whereas glucose and fructose accumulated to higher levels. This supports the hypothesis that sweetness loss during storage is primarily driven by sucrose hydrolysis into reducing sugars[26]. Accumulation of reducing sugars in VAC may also enhance Maillard and Strecker reactions, potentially promoting browning and off-flavor formation, although this requires further validation. In contrast, IQFP slowed sucrose degradation, providing a biochemical basis for sweetness retention and supporting recent findings on the central role of sugars in corn flavor stability[27].

Kernel metabolites are critical determinants of flavor, aroma, and nutritional value, and their dynamic changes directly influence product quality[28]. After 30 days, VAC exhibited marked reductions in umami-related amino acids such as glutamate and aspartate, whereas IQFP displayed metabolic features associated with stress response, including elevated zeatin and purine metabolites. During long-term storage, IQFP accumulated higher levels of protective sugars such as trehalose and oxidized lipid metabolites such as 13-HODE, whereas VAC accumulated metabolites linked to membrane degradation, bitterness, and oxidative stress, including hypoxanthine and sinapinic acid. These findings indicate that VAC storage is characterized by pronounced membrane lipid oxidation and protein degradation, whereas IQFP establishes a metabolomic pattern associated with stress protection and improved cellular stability. Such metabolite network alterations are closely linked to flavor changes[19]. This correlation is consistent with previous reports on waxy corn storage[29].

Maintaining authentic flavor under mild processing conditions has become increasingly important in response to consumer demand for natural foods[5]. Previous studies have explored how steaming, blanching, and low-temperature storage affect the quality of fruits and vegetables[9, 15, 21]. However, the dynamic impact of freezing prior to processing on the flavor stability of vacuum-packaged plant products remains poorly understood. This study demonstrates the superior long-term flavor stability of IQFP relative to VAC and reveals its underlying metabolic basis (Fig. 7). Nevertheless, limitations remain, as instrumental flavor analysis has not yet been validated by large-scale consumer sensory testing. Future work should integrate descriptive sensory analysis and consumer acceptance studies to link chemical flavor markers with human perception and develop predictive models for flavor quality.

Materials and Methods

Plant material preparation

Sweet corn (*Zea mays* L.), cv. 'Nongkenuo 336', was used in this study. Cultivation and harvesting conditions were consistent with those described in our previous work[30]. A total of 160 cobs with uniform weight (280–320 g), length (17–20 cm), and free of visible defects were selected and randomly assigned to two treatment groups. For the VAC group (immediate postharvest processing), the corn was husked, silk was removed, and both ends were trimmed to eliminate inedible portions. The ears were rinsed under purified running water, blanched in hot water at 95°C for 15 min, and cooled to room temperature. Samples were then vacuum-sealed in high-barrier retort pouches (PA/RCPP) and sterilized at 121°C for 20 min using an autoclave. For the IQFP group (Freezing storage prior to processing), fresh corn ears were immediately frozen at -20°C and stored for 30 d. After thawing, samples were processed using the same procedure described for the VAC group and subsequently subjected to storage analysis. All VPSC samples were stored in a constant-temperature chamber at 25°C. Sampling was conducted immediately after processing (CK-0d) and after 30, 60, 90, and 120 days of storage.

Sensory evaluation, color measurement, and texture profile analysis

Sensory evaluation was performed according to the method of Liu *et al.*[31] with minor modifications. A trained panel consisting of ten assessors (five males and five females) evaluated the samples independently based on the scoring criteria presented in (Supplementary Table S6).

Color parameters were measured using a calibrated colorimeter following Liu *et al.*[31] Three ears from each group were selected, and measurements were taken at three central points on the kernel surface to obtain *L**, *a**, and *b** values, representing lightness, redness–greenness, and yellowness-blueness, respectively.

Texture profile analysis was performed using a CT3 texture analyzer (AMETEK Brookfield, USA). Samples were subjected to a double-compression test using a P/50 probe to simulate mastication. The test

parameters were: compression depth 6.0 mm, test speed 1.0 mm s^{-1}, interval between compressions 10 s, and trigger force 10 g. Hardness, springiness, cohesiveness, and chewiness were calculated automatically by the instrument software to quantitatively characterize textural properties.

Determination of sugars

Sample preparation followed Zhao *et al.*[32] with minor modifications. Briefly, 20 mg of corn kernel powder was transferred into a centrifuge tube and extracted with 500 µL methanol: isopropanol: water (3:3:2, v/v/v). The mixture was vortexed for 3 min and ultrasonicated in a water bath at 4°C for 30 min. After centrifugation at 12,000 rpm for 3 min at 4°C, 50 µL of the supernatant was collected and mixed with 20 µL internal standard solution (1000 µg mL^{-1}). The extract was concentrated under nitrogen, freeze-dried, and derivatized with 100 µL methoxyamine hydrochloride in pyridine (15 mg mL^{-1}) at 37°C for 2 h, followed by reaction with 100 µL BSTFA at 37°C for 30 min. The derivatized solution (50 µL) was diluted to 1 mL with *n*-hexane, filtered through a 0.22 µm membrane, and transferred to an amber vial for GC-MS analysis.

GC-MS analysis followed Sun *et al.*[33] with minor modifications. A DB-5MS column (30 m × 0.25 mm × 0.25 µm) was used. Injection volume was 1 µL with a split ratio of 5:1. Helium was used as carrier gas at 1 mL min^{-1}. The oven temperature program was: 160°C for 1 min, ramped to 200°C at 6°C min^{-1}, then to 270°C at 10°C min^{-1}, and finally to 320°C at 20°C min^{-1} with a 5.5 min hold. Transfer line temperature was 280°C, ion source temperature 230°C, quadrupole temperature 150°C, and electron ionization energy 70 eV. Data were acquired in SIM mode with a solvent delay of 4 min.

Widely targeted metabolomics analysis

Widely targeted metabolomics was performed using an ultra-performance liquid chromatography–tandem mass spectrometry (UPLC-MS/MS) system following Liu *et al.*[34] Extracts were separated on a Waters HSS-T3 column. The mobile phase consisted of water containing 0.1% formic acid and 5 mM ammonium acetate (A) and acetonitrile containing 0.1% formic acid (B) under gradient elution. Mass spectrometry was performed using an electrospray ionization source operating in both positive and negative modes, and metabolites were quantified using multiple reaction monitoring (MRM).

Raw peak areas were normalized to total ion intensity. PCA and Spearman correlation analysis were used to assess sample reproducibility. Orthogonal partial least squares discriminant analysis (OPLS-DA) was applied to model metabolic differences, and model robustness was validated using 200 permutation tests. DAMs were screened using VIP > 1, $p < 0.05$, and fold change (FC) > 1. KEGG pathway enrichment analysis was performed using a hypergeometric test to identify significantly affected metabolic pathways[35].

HS-SPME-GC-MS analysis

A 0.2 g sample was placed into a headspace vial with 0.2 g NaCl and 20 µL internal standard solution (10 µg mL^{-1}). Analysis followed Yuan *et al.*[36] and Huang *et al.*[37] with minor modifications. For HS-SPME

extraction, samples were incubated at 60°C for 5 min. A 120 μm DVB/CWR/PDMS SPME-Arrow fiber was exposed to the headspace for 15 min, and volatile compounds were desorbed in the GC inlet at 250°C for 5 min. GC-MS conditions were as follows: helium carrier gas at 1.2 mL min^{-1}; injector temperature 250°C. The oven temperature program was: 40°C for 3.5 min, ramped to 100°C at 10°C min^{-1}, then to 180°C at 7°C min^{-1}, and finally to 280°C at 25°C min^{-1} with a 5 min hold. Electron ionization was performed at 70 eV, with ion source and quadrupole temperatures of 230°C and 150°C, respectively. Data were acquired in SIM mode.

ROAV analysis followed Huang *et al.*[37] PCA was conducted using the prcomp function in R. Hierarchical clustering heatmaps were generated, and Pearson correlation coefficients were calculated using the cor function. DVMs were defined as VIP > 1 and $|\log_2 FC| \geq 1$. Metabolite annotation was performed using the KEGG compound database.

Electronic nose analysis

Electronic nose analysis followed Tao *et al.*[38] with minor modifications. A 2.0 g sample was placed in a 20 mL headspace vial and sealed, then incubated at 95°C for 15 min to release volatile compounds. Detection was conducted using a PEN3 electronic nose (Airsense, Germany). Operating parameters were: sampling interval 1 s, pre-purge time 120 s, zero adjustment 10 s, pre-sampling time 5 s, measurement time 150 s, and injection flow rate 350 mL min^{-1}. Each sample was analyzed in triplicate, and stable sensor responses between 102–104 s were used for statistical analysis.

GC-IMS analysis

GC-IMS analysis was performed using a FlavourSpec® system (G.A.S., Germany) following Tao *et al.*[38] with modifications. A 2.0 g sample was sealed in a 10 mL headspace vial and incubated at 95°C for 15 min. Separation was achieved on an MXT-5 column (15 m × 0.53 mm, 1 μm). Headspace needle temperature was 85°C and injection volume 500 μL. GC conditions were: column temperature 60°C; carrier gas nitrogen (≥ 99.999%); initial flow 2 mL min^{-1} for 2 min, increased to 10 mL min^{-1} over 8 min, then to 100 mL min^{-1} over 10 min, and finally to 150 mL min^{-1} over 10 min. IMS conditions were: drift gas flow 150 mL min^{-1}; detector temperature 45°C; total run time 31 min. Volatile compound identification and sensory annotation were performed using the Food Flavor Laboratory (http://foodflavorlab.cn/#/v2/home), NCBI, and FEMA (https://www.femaflavor.org/) databases.

Statistical analysis

All experiments were conducted with three biological replicates. Data were processed using Excel. Statistical analysis was performed using IBM SPSS Statistics 27. One-way analysis of variance (ANOVA) followed by the least significant difference (LSD) test was used to evaluate differences among groups. Differences were considered significant at $p < 0.05$ and highly significant at $p < 0.01$. Figures were generated using WPS Office, Metware Cloud, and CNSknowall.

Data availability

Data is provided within the manuscript or Additional information files.

Declarations

Acknowledgements

This study was supported by Beijing Innovation Consortium of Agriculture Research System (BAIC02-2026); the Beijing Rural Revitalization Agricultural Science and Technology Project (NY2401120324; NY2602740126); BAAFS Foundation for Excellent Young Scientists (Grant No.YKPY202614)

Author contributions

Yanyan Zheng, Jinhua Zuo, and Yunxiang Wang conceived and designed the experiment. Hua Chen, Xinyuan Zhou, Tianyu Li, Xu Liu, Yiting Ren, Xinyi Feng, Chunmei Bai, and Jiejie Tao performed all experiments and storage samplings. Jinhua Zuo, Yanyan Zheng, Lihong Wang, Yunxiang Wang, Ronghuan Wang, and Yaxing Shi were responsible for supervision, funding acquisition, and resources provision. Hua Chen and Jinhua Zuo drafted the initial manuscript. Yanyan Zheng critically reviewed and edited the manuscript. All authors read and approved the manuscript.

Competing interests

The authors declare no competing interests.

Ethical approval

The research described in this paper have been performed in accordance

with the Declaration of Helsinki, and applicable ethical principles and legal

regulations. All the tasters who participated in the examination provide

informed consent before the sensory examination began.

Additional information

Supplementary Material **Figures S1-9**; Supplementary Material **Tables S1-6**. The online version contains supplementary material available at

References

1. Sun, G. *et al*. Effect of roasting treatment on flavor and quality of fragrant corn oil. *Food Chem* 492, 145426 (2025). https://doi.org/10.1016/j.foodchem.2025.145426
2. Liu, S. *et al*. Storage temperature affects metabolism of sweet corn. *Postharvest Biol Tec* 219 (2025). https://doi.org/10.1016/j.postharvbio.2024.113232

3. Zhu, G., Gou, J., Klee, H. & Huang, S. Next-gen approaches to flavor-related metabolism. *Annu Rev Plant Biol* 70, 187–212 (2019). https://doi.org/10.1146/annurev-arplant-050718-100353
4. Garg, N. *et al*. FlavorDB: a database of flavor molecules. *Nucleic Acids Res* 46, D1210-D1216 (2018). https://doi.org/10.1093/nar/gkx957
5. Bel-Rhlid, R., Berger, R. G. & Blank, I. Bio-mediated generation of food flavors -Towards sustainable flavor production inspired by nature. *Trends Food Sci Technol* 78, 134–143 (2018). https://doi.org/10.1016/j.tifs.2018.06.004
6. Li, T. *et al*. Ozone treatment maintains the sweetness and volatile odor of sweet corn by enhancing antioxidant capacity and resistance to disease. *Postharvest Biol Tec* 231 (2026). https://doi.org/10.1016/j.postharvbio.2025.113947
7. Gong, P. *et al*. Comparative assessment of storage conditions on vacuum-packaged ready-to-eat corn: temporal changes in physicochemical parameters and sensory quality. *J Food Sci* 90, e70722 (2025). https://doi.org/10.1111/1750-3841.70722
8. Li, Y. *et al*. Sensory evaluation and model prediction of vacuum-packed fresh corn during long-term storage. *Foods* 12 (2023). https://doi.org/10.3390/foods12030478
9. Onyeaka, D. H., Nwaizu, C.-C. & Ekaette, I. Mathematical modeling for thermally treated vacuum-packaged foods: A review on sous vide processing. *Trends Food Sci Technol* 126, 73–85 (2022). https://doi.org/10.1016/j.tifs.2022.06.018
10. Farag, M. A., Ammar, N. M., El Gendy, A. N. & Mohsen, E. Effect of grilling as processing method on Zea mays (corn) metabolites composition as analyzed via SPME GC-MS and chemometrics. *J Food Process Preserv* 43 (2019). https://doi.org/10.1111/jfpp.14165
11. Stonehouse, G. G. & Evans, J. A. The use of supercooling for fresh foods: A review. *J Food Eng* 148, 74–79 (2015). https://doi.org/10.1016/j.jfoodeng.2014.08.007
12. Liu, D.-K., Xu, C.-C., Guo, C.-X. & Zhang, X.-X. Sub-zero temperature preservation of fruits and vegetables: A review. *J Food Eng* 275 (2020). https://doi.org/10.1016/j.jfoodeng.2019.109881
13. Fan, Z. *et al*. Effect of liquid nitrogen spray quick-freezing technology on the quality of bamboo shoots, Dendrocalamus brandisii from Yunnan Province, China. *J Food Eng* 368 (2024). https://doi.org/10.1016/j.jfoodeng.2023.111916
14. Mao, C. *et al.* Freezing pre-treatment improves radio frequency explosion puffing (RFEP) quality by altering the cellular structure of purple sweet potato [*Ipomoea batatas* (L) Lam.]. *Food Res Int* 184, 114265 (2024). https://doi.org/10.1016/j.foodres.2024.114265
15. Xin, Y., Zhang, M., Xu, B., Adhikari, B. & Sun, J. Research trends in selected blanching pretreatments and quick freezing technologies as applied in fruits and vegetables: A review. *Int J Refrig* 57, 11–25 (2015). https://doi.org/10.1016/j.ijrefrig.2015.04.015
16. Jia, X., Katsuno, N. & Nishizu, T. Effects of temperature fluctuations on the development of surface sugar crystals and the quality characteristics of dried persimmon during frozen storage. *Food Bioprocess Technol* 15, 561–570 (2022). https://doi.org/10.1007/s11947-021-02750-8

17. Colantonio, V. *et al*. Metabolomic selection for enhanced fruit flavor. *Proc Natl Acad Sci U S A* 119 (2022). https://doi.org/10.1073/pnas.2115865119
18. Spence, C. Multisensory flavor perception. *Cell* 161, 24–35 (2015). https://doi.org/10.1016/j.cell.2015.03.007
19. Luo, J. *et al*. A metabolic roadmap of waxy corn flavor. *Mol Plant* 17, 1883–1898 (2024). https://doi.org/10.1016/j.molp.2024.11.003
20. Ma, S. *et al*. NaCl treatment with low density polyethylene packaging bags can enhance the aroma of fresh-cut apple, not only inhibit its browning. *Food Packag Shelf Life* 39 (2023). https://doi.org/10.1016/j.fpsl.2023.101148
21. Wang, M., Jin, S., Ding, Z. & Xie, J. Effects of different freezing methods on physicochemical properties of sweet corn during storage. *Int J Mol Sci* 24 (2022). https://doi.org/10.3390/ijms24010389
22. Brenner, M. P. & Sorensen, P. M. Biophysics of molecular gastronomy. *Cell* 161, 5–8 (2015). https://doi.org/10.1016/j.cell.2015.03.002
23. Xie, X. *et al*. Characterization and metabolism pathway of volatile compounds in blueberries of different varieties and origins analyzed via HS-GC-IMS and HS-SPME-GC-MS. *Food Chem* 480, 143813 (2025). https://doi.org/10.1016/j.foodchem.2025.143813
24. Xu, D. *et al*. Vacuum packaging and ascorbic acid synergistically maintain the quality and flavor of fresh-cut potatoes. *Lwt* 162 (2022). https://doi.org/10.1016/j.lwt.2022.113356
25. Cha, J. Y. *et al*. Variation of volatile compounds and sensory profile for Protaetia brevitarsis larvae fermented with lactic acid bacteria and yeast. *Food Chem* 452, 139480 (2024). https://doi.org/10.1016/j.foodchem.2024.139480
26. Calvo-Brenes, P. & O´Hare, T. Effect of freezing and cool storage on carotenoid content and quality of zeaxanthin-biofortified and standard yellow sweet-corn (Zea mays L.). *J Food Compost Anal* 86 (2020). https://doi.org/10.1016/j.jfca.2019.103353
27. Chen, S. *et al*. Unravelling the postharvest quality diversities of different sweet corn varieties. *Postharvest Biol Tec* 209 (2024). https://doi.org/10.1016/j.postharvbio.2023.112718
28. He, Y. *et al*. Effects of steaming on fresh edible kernels of waxy and normal maize determined by metabolomic analysis. *Foods* 13 (2024). https://doi.org/10.3390/foods13244157
29. Li, C. *et al*. Large-scale metabolomic landscape of edible maize reveals convergent changes in metabolite differentiation and facilitates its breeding improvement. *Mol Plant* 18, 619–638 (2025). https://doi.org/10.1016/j.molp.2025.02.007
30. Chen, H. *et al*. Effects of low-voltage electrostatic field on post-harvest sugar metabolism and stress resistance in sweet corn. *Postharvest Biol Tec* 231 (2026). https://doi.org/10.1016/j.postharvbio.2025.113859
31. Liu, S. *et al*. Chlorine dioxide affects metabolism of harvested sweet corn. *Postharvest Biol Tec* 211 (2024). https://doi.org/10.1016/j.postharvbio.2024.112834

32. Zhao, C. *et al*. Arabinose biosynthesis is critical for salt stress tolerance in Arabidopsis. *New Phytol* 224, 274–290 (2019). https://doi.org/10.1111/nph.15867
33. Sun, S., Wang, H., Xie, J. & Su, Y. Simultaneous determination of rhamnose, xylitol, arabitol, fructose, glucose, inositol, sucrose, maltose in jujube (Zizyphus jujube Mill.) extract: comparison of HPLC-ELSD, LC-ESI-MS/MS and GC-MS. *Chem Cent J* 10, 25 (2016). https://doi.org/10.1186/s13065-016-0171-2
34. Liu, S. *et al*. Mechanism of vacuum packaging regulating postharvest quality of Mopan persimmon. *Food Qual Saf* 9 (2025). https://doi.org/10.1093/fqsafe/fyaf024
35. Bai, C. *et al*. Multiomics analyses of the effects of LED white light on the ripening of apricot fruits. *J Adv Res* 67, 1–13 (2025). https://doi.org/10.1016/j.jare.2024.01.008
36. Yuan, H. *et al*. WTV2.0: A high-coverage plant volatilomics method with a comprehensive selective ion monitoring acquisition mode. *Mol Plant* 17, 972–985 (2024). https://doi.org/10.1016/j.molp.2024.04.012
37. Huang, D. *et al*. A comprehensive metabolomics analysis of volatile and non-volatile compounds in matcha processed from different tea varieties. *Food Chem X* 21, 101234 (2024). https://doi.org/10.1016/j.fochx.2024.101234
38. Tao, J. *et al*. Low storage temperature affects quality and volatile compounds in fresh tomatoes. *Food Chem* 460, 140400 (2024). https://doi.org/10.1016/j.foodchem.2024.140400

Figures

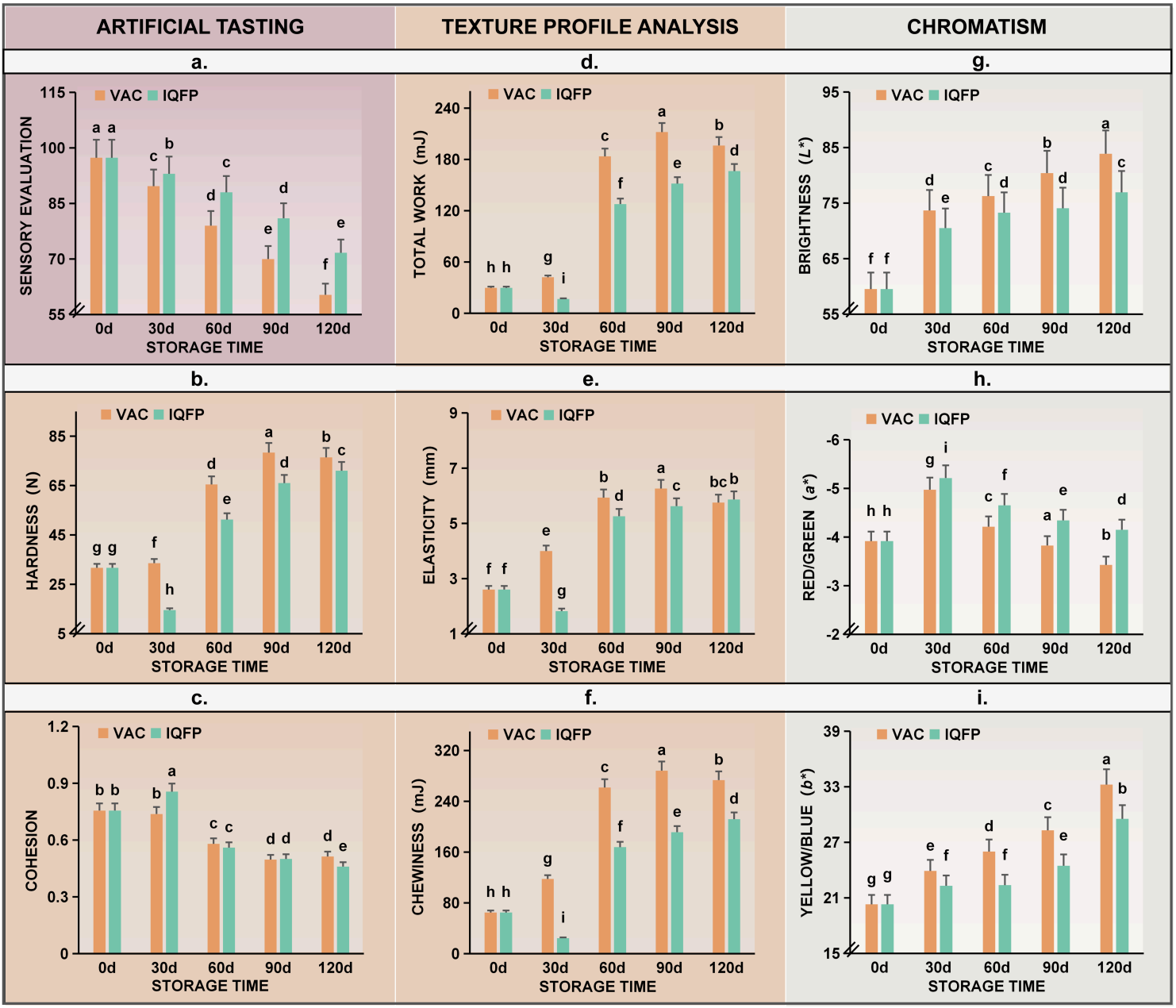

Figure 1

Comparison of sensory and texture characteristics of vacuum-packed sweet corn during storage: **(a)** sensory evaluation; **(b-f)** texture profile analysis; **(g-i)** color difference analysis of samples VAC versus those IQFP.

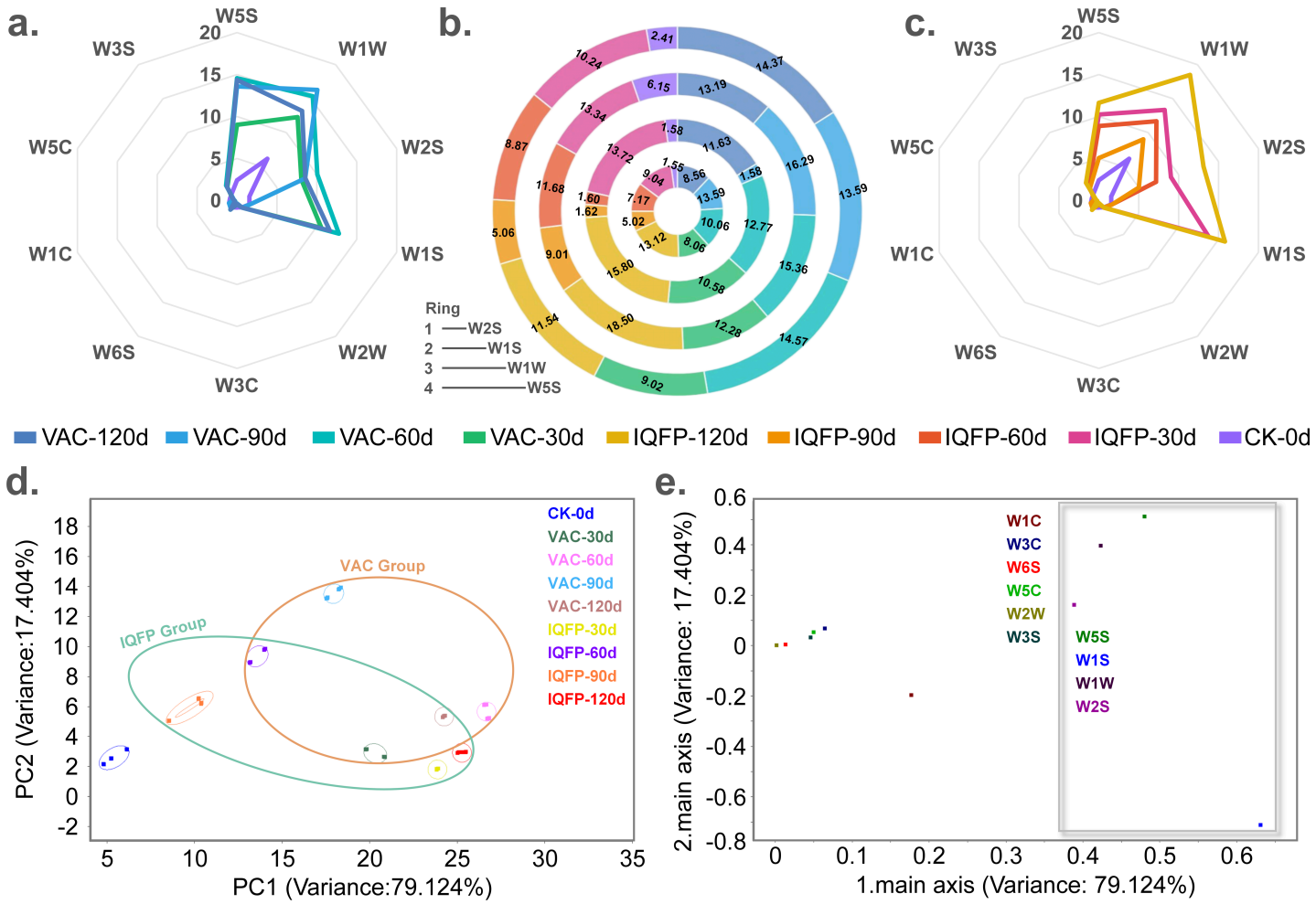

Figure 2

Electronic nose analysis of VPSC: **(a, c)** radar chromatograms; **(b)**changes in flavor ring during storage; **(d)** principal component analysis; **(e)** loading analysis of the electronic nose.

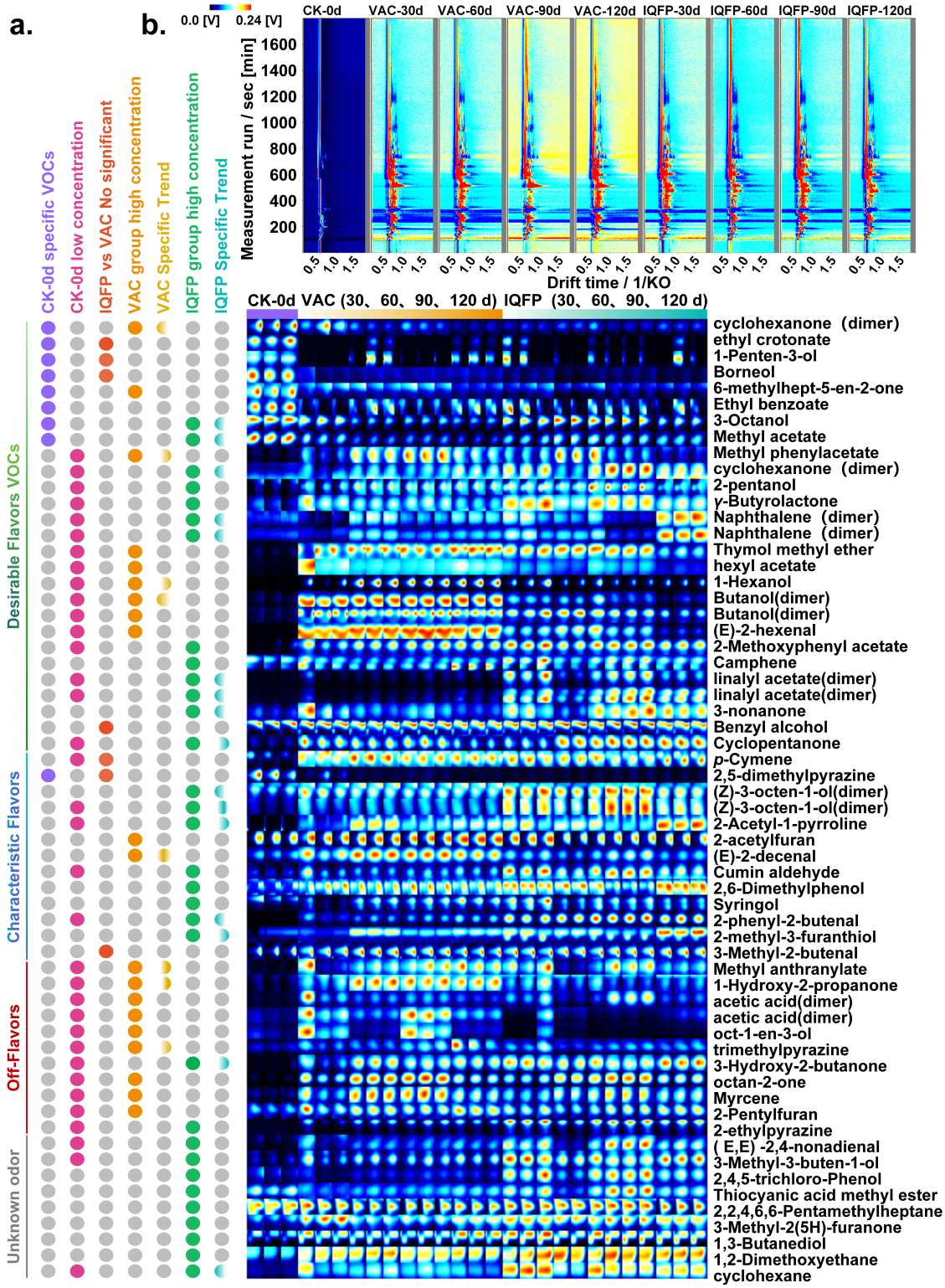

Figure 3

Analysis of VPSC by GC-IMS: **(a)** flavor fingerprint profile of vacuum-packed sweet corn; **(b)**two-dimensional comparative plots of VAC and IQFP groups after background subtraction of CK-0d.

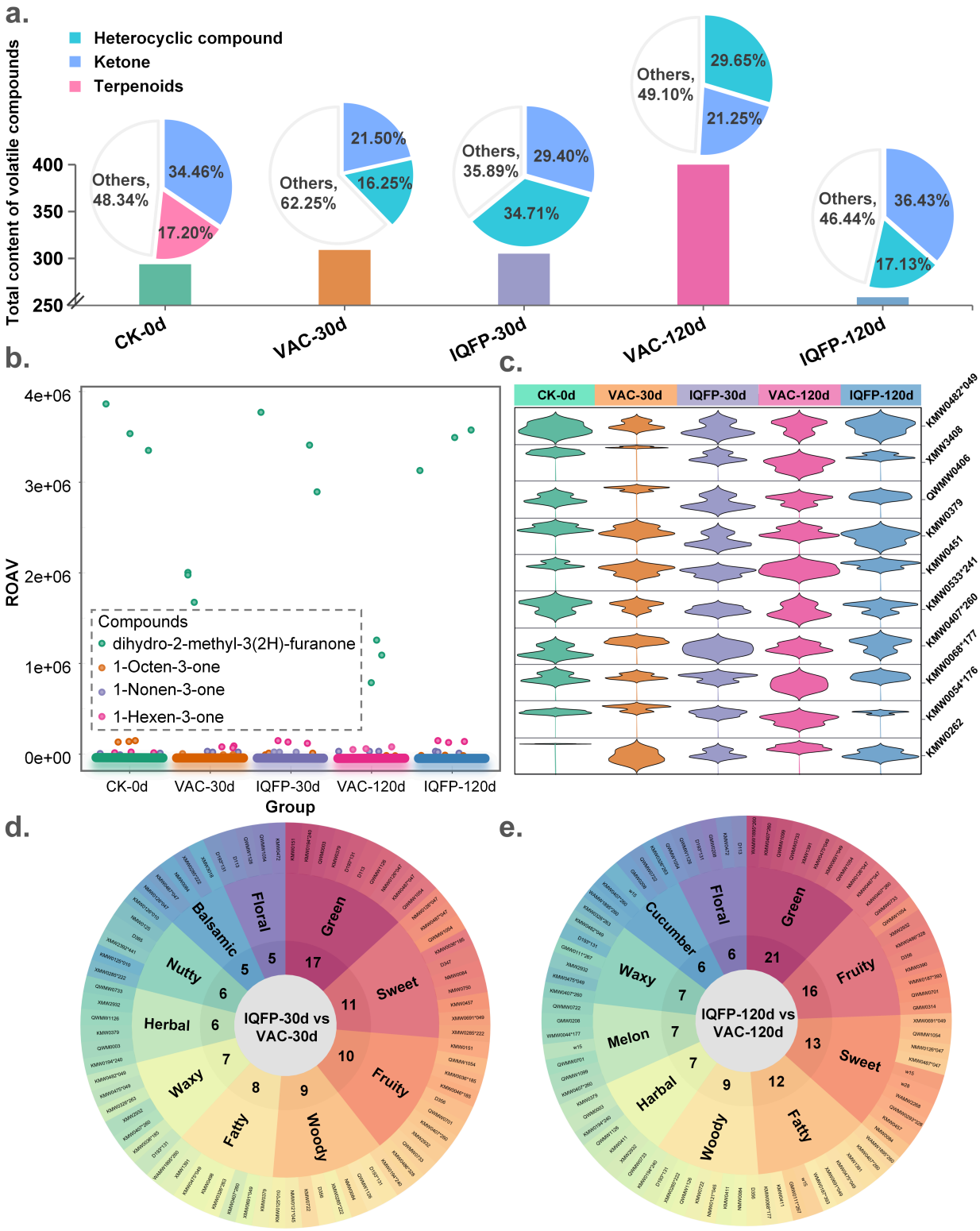

Figure 4

Analysis of differential volatile metabolites (DVMs): **(a)** Bar chart showing the total content of DVMs in each sample, with a nested pie chart illustrating the two compounds with the highest proportions; **(b)** Scatter plot of DVMs based on ROAV; **(c)** Violin plots concentrations of 10 DVMs, with rows representing metabolites and columns representing groups; **(d-e)**Flavor wheel analysis of DVMs identified under short-term and long-term storage conditions, respectively. The wheel comprises three rings: the third ring

lists the top 10 sensory flavor attributes; the second ring shows the count of DVMs associated with each attribute; and the outermost ring displays the DVMs ranked within the top 10 by VIP score.

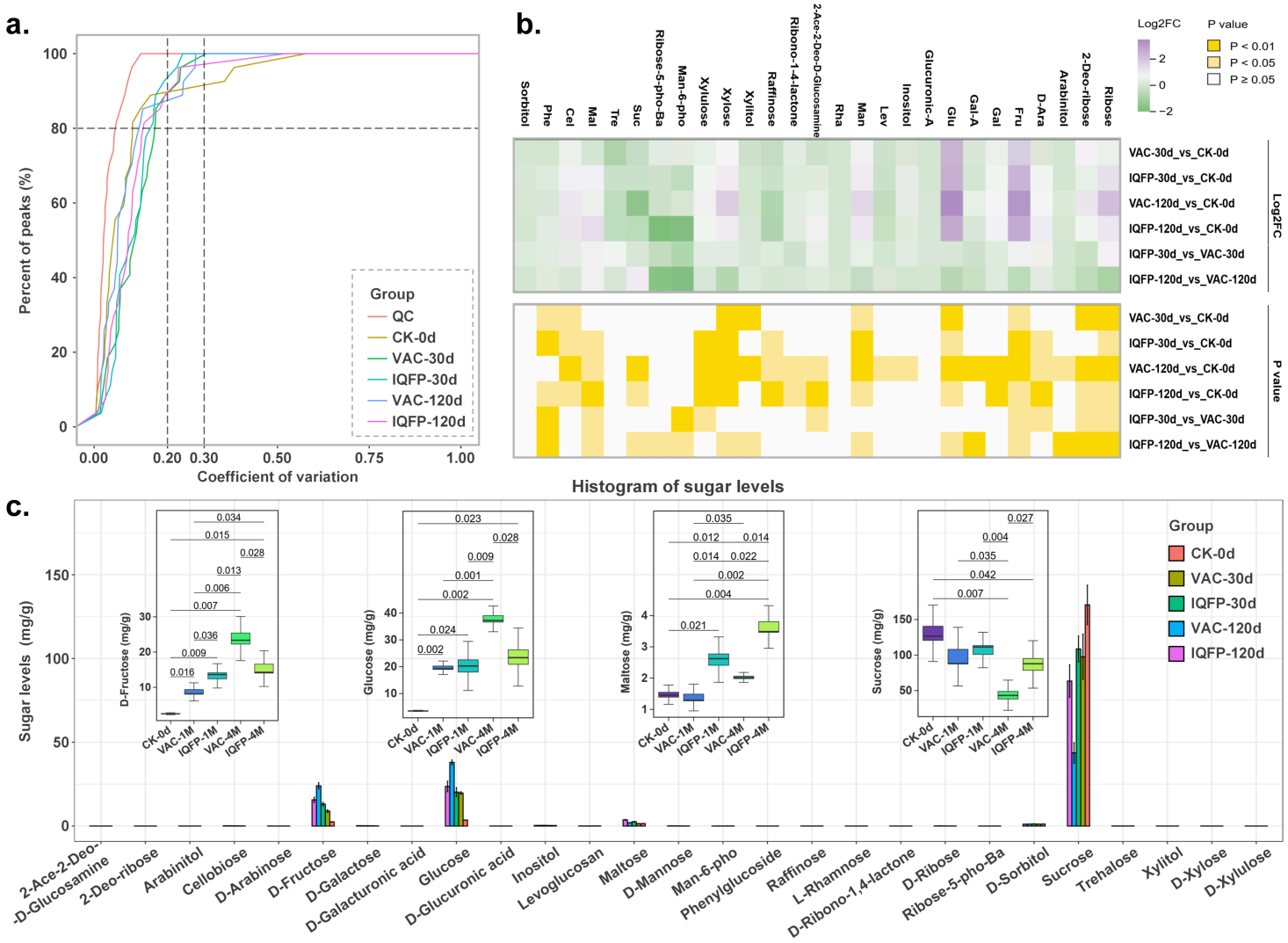

Figure 5

Quantitative analysis of sugars: **(a)** Distribution of coefficient of variation values for sugars in QC samples; **(b)** cluster heatmap analysis of 27 sugars across different comparison groups; **(c)** histogram of sugar levels, with embedded box plots showing the results of significance tests for the four most abundant sugars.

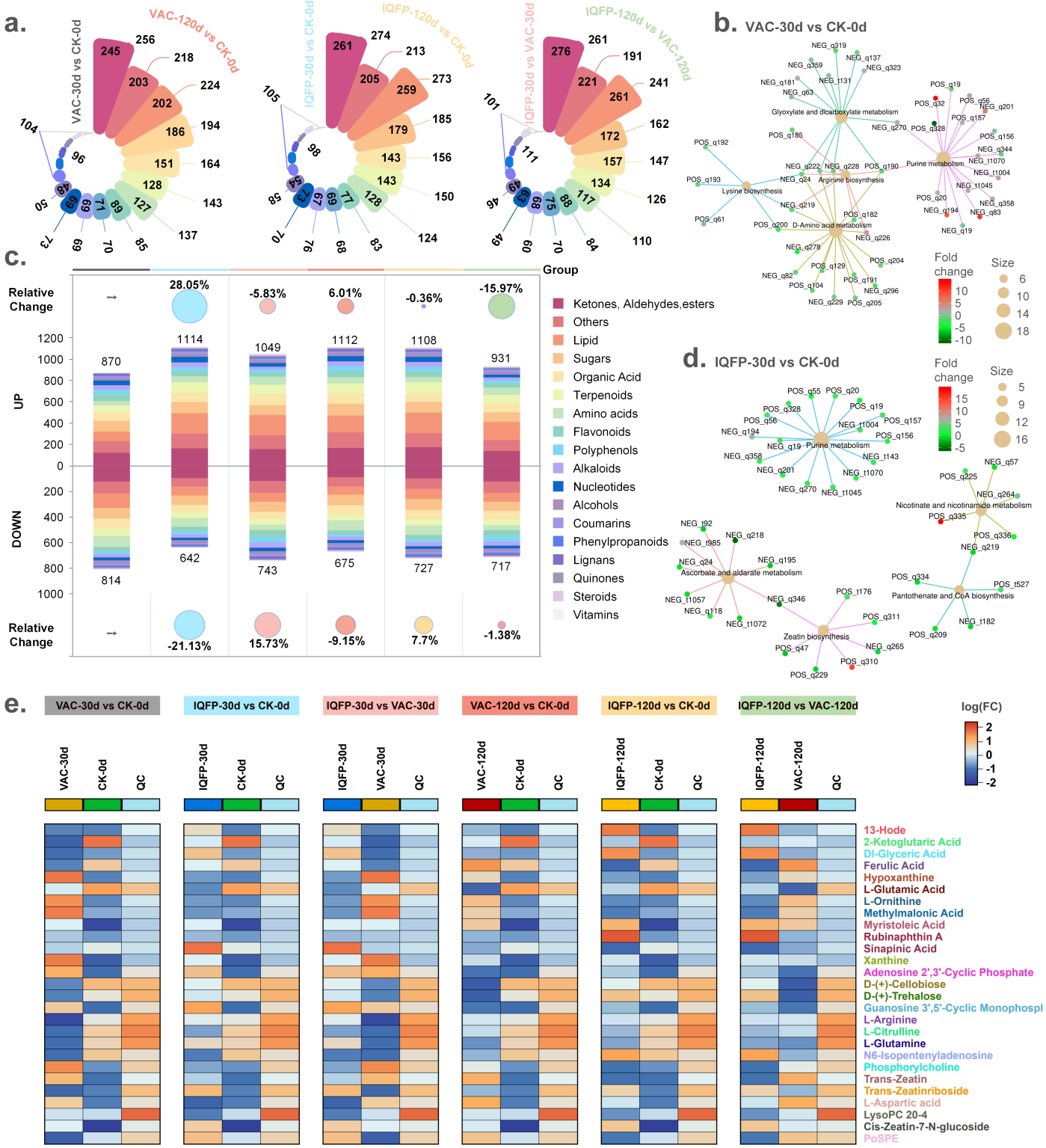

Figure 6

Analysis of differentially accumulated metabolites (DAMs). **(a)** Rose diagram showing the distribution of DAMs categories across different comparison groups; **(b, d)** Network analysis of the top five significantly enriched KEGG pathways in each comparison group; **(c)** Stacked bubble plot illustrating the numbers of upregulated, downregulated, and total DAMs across comparison groups; **(e)** Batch matrix heatmap displaying expression patterns of 27 key DAMs in each comparison group.

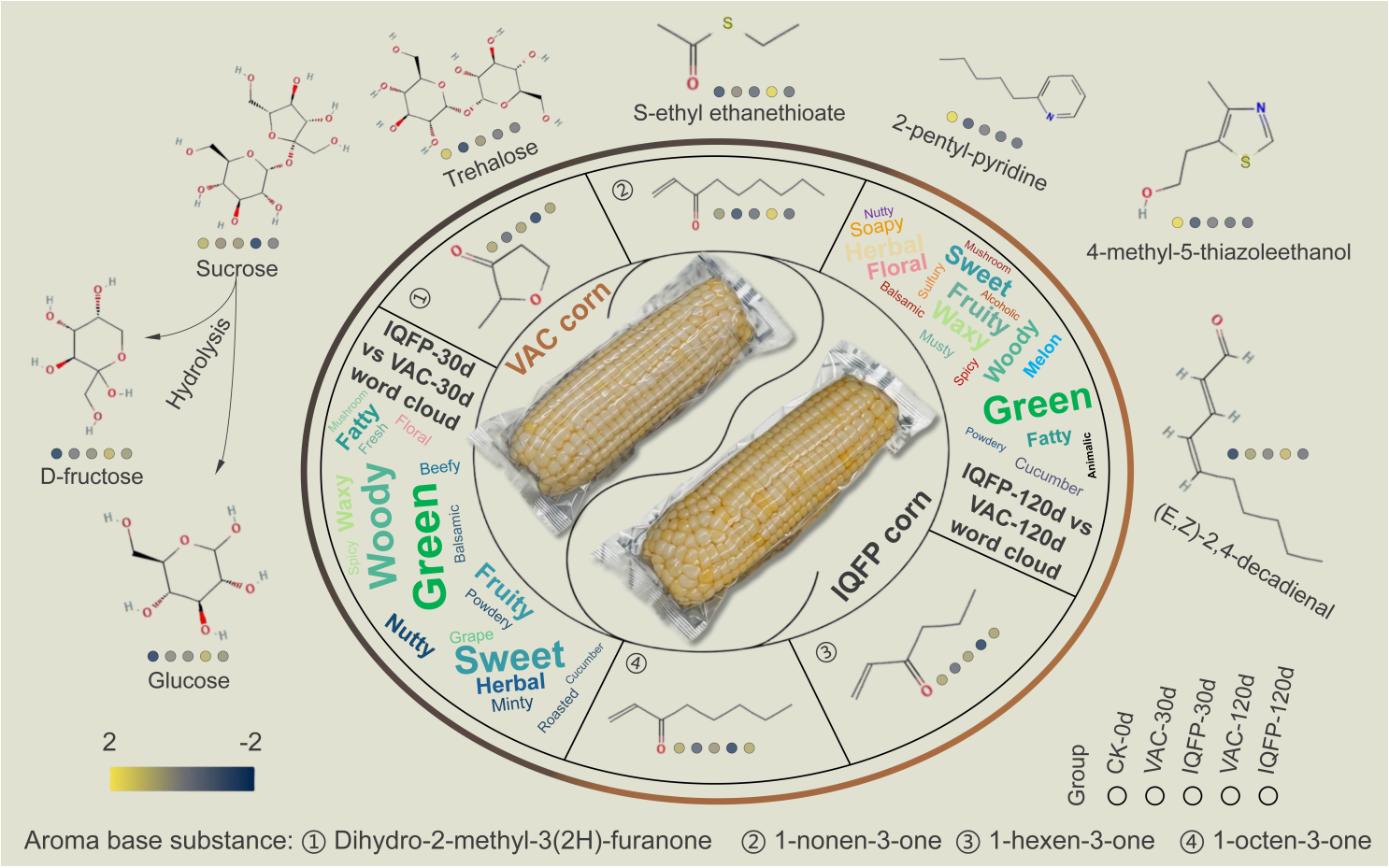

Figure 7

Model of the effects of Freezing Storage Prior to Processing on Flavor and Nutritional Quality of Vacuum-Packed Sweet Corn.

Supplementary Files

This is a list of supplementary files associated with this preprint. Click to download.

- SupplementaryTablesS16.docx
- SupplementaryFiguresS19.docx